iJRASET
International Journal For Research in
Applied Science and Engineering Technology

INTERNATIONAL JOURNAL FOR RESEARCH

IN APPLIED SCIENCE & ENGINEERING TECHNOLOGY

Volume: 11 **Issue:** XII **Month of publication:** December 2023

DOI: https://doi.org/10.22214/ijraset.2023.57471

International Journal for Research in Applied Science & Engineering Technology (IJRASET)
ISSN: 2321-9653; IC Value: 45.98; SJ Impact Factor: 7.538
Volume 11 Issue XII Dec 2023- Available at www.ijraset.com

Seismic Analysis of High-Rise Building using Negative Stiffness Device

Shubham Waghchaure[1], Dr. Manisha Waghmare[2]
[1]P.G. Student, Dept. of Civil Engineering, AISSMS College of Engineering, Pune, India
[2]Prof. Dept. of Civil Engineering, AISSMS College of Engineering, Pune, India

***Abstract:** Natural hazard mitigation is one of the most important issues facing civil engineers today. In structural engineering, one of the constant challenges is to find new and better means of protecting existing and new civil structures from the damaging effects of destructive environmental forces, such as wind, waves and earthquakes. Earthquakes are considered the most destructive environmental forces for civil engineering structures. Seismic forces and displacements in existing structures can be effectively reduced in an approach where the structure is intentionally weakened (stiffness and strength are reduced) and damping is added. However, the approach also results in inelastic excursions and permanent deformation of the structural system during a seismic event. A new concept previously proposed by the authors simulates apparent weakening by incorporating a mechanical system that produces true negative stiffness in the structural system. In doing so, inelastic excursions and permanent deformations may be substantially reduced or eliminated. True negative stiffness means that the force must assist motion, not oppose it as in the case of a positive stiffness spring. A passive device capable of exhibiting true negative stiffness, negative stiffness device (NSD), without external power supply is studied in this project work. A pre-compressed spring is used to generate the force to push the structure and a lever-mechanism is adapted to amplify the generated force.*

In the present approach an attempt has been made to study an inelastic multistoried RCC building to demonstrate the effectiveness of placing NSDs at multiple locations along the height of the building; referred to as "Distributed Isolation" and also by placing NSD's at base of the building; referred to as "Base Isolation". By performing nonlinear dynamic analysis, the different parameters which will act as a measure of seismic performance of RCC building such as Base Shear, Top Acceleration, Top Displacement and Column Force are studied.

***Keywords:** Negative stiffness device, Base isolation, Distributed Isolation.*

I. INTRODUCTION

A. Negative Stiffness Device

True negative stiffness means that the force must assist motion, not oppose it as in the case of a positive stiffness spring. True negative stiffness needs no external power supply. A pre-compressed spring is used to generate the force to push the structure and a lever-mechanism is adapted to amplify the generated force. The reason that this technology has been restricted to small mass applications is the large forces required to develop the necessary negative stiffness. These preload forces are typically on the order of the weight of the isolated structure. The application of negative-stiffness concept to massive structures, such as buildings and bridges, requires modification of the existing mechanisms to reduce the demand for preload force and to package the negative stiffness device in a system that does not impose any additional loads on the structure, other than those needed for achieving the goal of seismic protection.

These requirements lead to the development of the true negative system device (NSD), which has the following components and characteristics:

1) A highly compressed machined spring (CS) that develops the force in the direction of motion (thus, negative stiffness); the magnitude of the force reduces with increasing displacement so that stability of the system is ensured at large displacements;
2) A double chevron self-containing system to resist the preload in the compressed spring and also to prevent the transfer of the vertical component of the preload to the structure;
3) A double negative stiffness magnification mechanism that substantially reduces the requirement for preload so that a practical system is achieved;

International Journal for Research in Applied Science & Engineering Technology (IJRASET)
ISSN: 2321-9653; IC Value: 45.98; SJ Impact Factor: 7.538
Volume 11 Issue XII Dec 2023- Available at www.ijraset.com

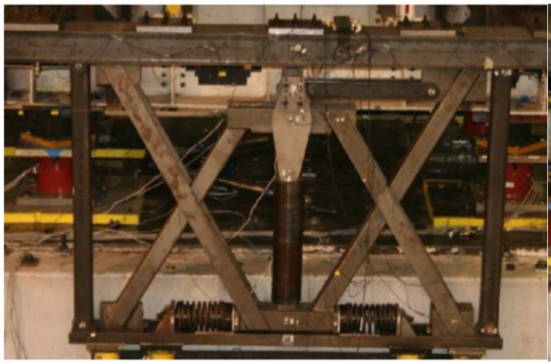
Fig.1.1 Undeformed NSD


Fig.1.2 Deformed NSD

4) A system (the GSA) that provides positive stiffness up to a predefined displacement such that the combined effective stiffness of CS and GSA is almost zero up to the predefined displacement; GSA is essential to simulate a bilinear elastic behavior with an apparent-yield displacement which is smaller than the actual yield displacement of the structure; and
5) Viscous damping devices in parallel with the negative stiffness device to reduce displacement demands to within acceptable limits.

In order to visualize the effect of adding true negative stiffness to a structure where viscous dampers and negative stiffness devices have been added, consider the force-displacement relations shown in Figure 1-1(a) (the dashed line is the force-displacement relation for the structure, the dotted line is the force-displacement relation for the viscous damper and the solid line is the force-displacement relation for the negative stiffness device). By adding the NSD to the structure, as schematically shown in Figure 1-1(b), the assembly stiffness reduces from the value K_e to $K_a = K_e - K_n$ for displacements beyond the limit $u_y{}'$. If, F_2 and u_2 are the maximum restoring force and maximum displacement of a perfectly-linear system (dashed line in Figure 1-1(b)) then for the same excitation, the maximum restoring force and the maximum displacement of the assembly of the structure and NSD are F_3 and u_3, respectively. Stiffness K_n is selected to achieve the desired reduction in base shear. Although a reduction in base shear is achieved, the maximum deformation of the system may increase when compared to the system without the NSD. Reduction of displacements to acceptable levels is achieved by adding passive damping devices in parallel to the NSD, as schematically shown in Figure 1-1(c). To demonstrate the concept, a linear viscous damper is used. The maximum displacement is reduced, resulting in $u'_3 < u_2$.

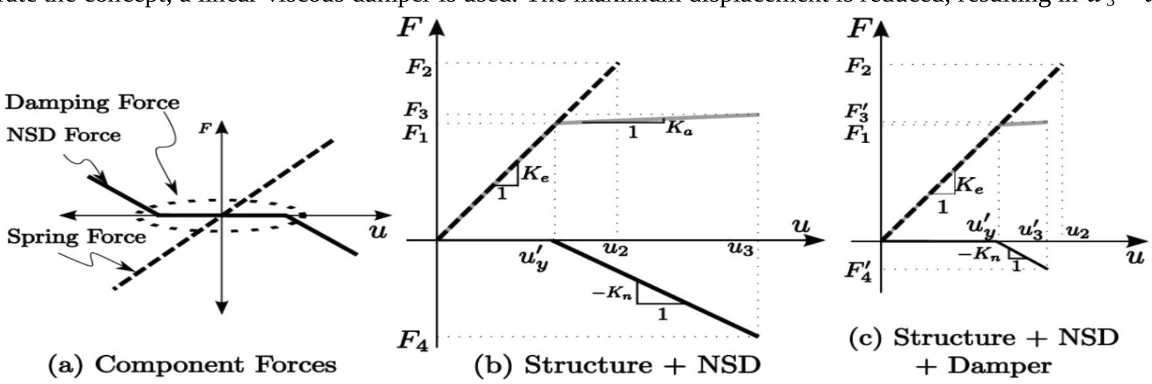

Fig. 1.3 Working principle of NSD

B. Operation of NSD

The NSD shown in Figure 1.4 is composed of a pre-compressed spring shown in the center of the device as well as the gap spring assemblies on the bottom. A combination of frame elements and plates hold these pieces together. When the device deforms, the pre-compressed spring is the one that creates the force that assists the motion or the negative force and thus the name negative stiffness for the device. The bottom spring assemblies (gap spring assembly mechanism) provide the device inherently with a bilinear elastic positive stiffness in order to make the device engage at larger displacements More specifically, around equilibrium, the positive stiffness caused by the gap spring assembly mechanism, cancels out the negative stiffness caused by the pre-compressed spring so that essentially the force/stiffness generated by the device is close to zero. After a prescribed displacement, the gap spring assembly softens drastically so that the pre-compressed spring acts essentially on its own creating the negative stiffness.

It is noted that the operation of the gap spring assembly is achieved without any yielding so that there is no inherent permanent deformation in the device.

The NSD should be bolted to the bottom of floor and the top of NSD is connected to the ceiling of the floor using an end-angle assembly that will transfer only the horizontal forces. Any interstory structural deformation will result in the deformation of the top channel, Top chevron (CB2) and the lever-arm. Since the lever-arm is connected to the pivot plate (point-B) and the pivot plate is fixed at point-C, any deformation of point-B will result in rotation of pivot-plate about point-C. As a result, point-D will displace in the opposite direction to that of point-B. Also, the bottom of CS is connected to Top chevron (CB2), so, point-E will undergo same deformation as point-B. The total lateral deformation of the CS is magnified by comparison to the displacement of point A,

(a) by the ratio CD to BC and

(b) due to the movement of point E in the opposite direction to D.

Essentially, any deformation at the top of NSD will result in the horizontal deformation of CS both at the top and bottom; this is the dual amplification.

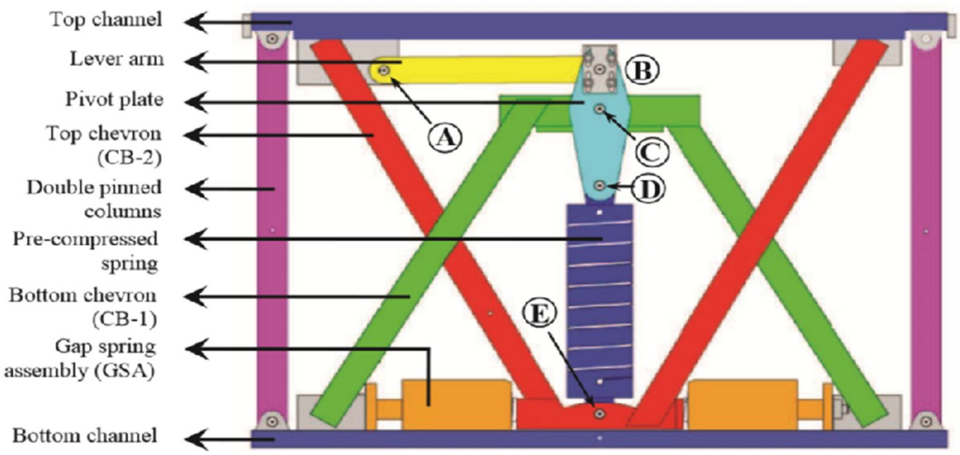

Fig.1.4 Schematic diagram of NSD

C. *Advantages of NSD*

1) The device changes the apparent global lateral stiffness of the structure, without changing the actual stiffness of the structure. The apparent stiffness is reduced to a very low-level simulating global lateral yielding without actual yielding in the main structure.
2) The device produces true horizontal negative stiffness by passively generating a force that assists the imposed displacement. No external power supply is needed since all the elements comprising the device are passive.
3) The device is self-contained and therefore when installed affects only the horizontal stiffness of the system while leaving the vertical stiffness intact. Stability and buckling limits of the structure are not affected. The NSD does not participate in transferring the vertical loads.
4) There is no significant hysteresis in the device. The NSD is essentially elastic.
5) The device provides variable stiffness which becomes positive at large deformations; therefore, its global behavior is “elastic nonlinear”. This is a desired feature as it promotes stability.
6) The device employs a double magnification mechanism that allows for easy adjustment of the negative stiffness value. The gap spring assembly (GSA) mechanism allows for adjustable gap opening.

D. *Mathematical Formulation of NSD*

In order to derive the force displacement equations of the device, by considering equilibrium of Negative Stiffness Damper following relationships are obtained by Nagarajaiah et al.

$$F_{NSD} = -\left(\frac{P_{in}+K_s l_p}{l_s} - K_s\right)\left(\frac{l_1}{l_2}\right)\left(2 + \frac{l_2}{l_1} + \frac{l_p+l_1}{\sqrt{l_2^2-u^2}}\right)u + F_g \qquad \dots (1.5.1)$$

ISSN: 2321-9653; IC Value: 45.98; SJ Impact Factor: 7.538
Volume 11 Issue XII Dec 2023- Available at www.ijraset.com

Table 1.1 *Properties of NSD and GSA used* [A. A. Sarlis and D. T. R. Pasala] (2013

Quantity	Symbol	Value	Units
Length BC of pivot plate	l_l	25.4	cm
Length CD of pivot plate	l_2	12.7	cm
NSD spring length	l_p	76.2	cm
NSD spring stiffness	K_s	1.4	kN/cm
NSD spring preload	P_{in}	16.5	kN
Double hinged column height	h	124.5	cm
Lever length	l_{lv}	67.3	cm
NSD engagement displacement	u'_y	1.65	cm
GSA spring S1 stiffness	k_{s1}	4.9	kN/cm
GSA spring S2 stiffness	k_{s2}	0.3	KN/cm
GSA spring S2 preload	P_{is2}	8.1	KN

Where, $F_g = \begin{cases} k_{s1}u, & 0 \le u \le u'_y \\ k_{s1}u'_y + k_{s2}(u - u'_y) & u > u'_y \end{cases}$ … (1.5.2)

From geometry and considering the fact that point C is fixed, the displacements of other points of the device are:

$u_B = u_E = u_D \frac{l_2}{l_1} = u$

The spring length at deformed configuration is given by:

$$l_s = \sqrt{\left(l_p + l_1 - l_1\sqrt{1 - \left(\frac{u}{l_2}\right)^2}\right)^2 + u^2\left(1 + \frac{l_1}{l_2}\right)^2}$$

E. Modeling of NSD In SAP2000

The NSD can be modelled in general purpose dynamic analysis programs in SAP2000v21 by direct modelling of the geometry of the device and its components and performing large displacement analysis. In this method the pre-compressed spring is modelled as a frame element (member DE in Figure 4.2) with a cross section area calculated so that it yields the stiffness of the spring in the axial direction. The moment of inertia of the spring should be very small but non zero. Frame elements that are perpendicular to the spring axis are connected at joints D and E and shown as $D - D$ " and $E - E$ " (E $- E$ " is not connected to the top chevron) respectively in Figure 4.2. These elements are used for the application of the preload. The preload is applied as external point element load (not joint load) in the local coordinate system of the frame elements directly at joints D and E without any eccentricity. The reason for using this procedure is that SAP2000 rotates the element loads together with the frame elements but it does not rotate joint loads together with the joints in large displacement analysis.

International Journal for Research in Applied Science & Engineering Technology (IJRASET)
ISSN: 2321-9653; IC Value: 45.98; SJ Impact Factor: 7.538
Volume 11 Issue XII Dec 2023- Available at www.ijraset.com

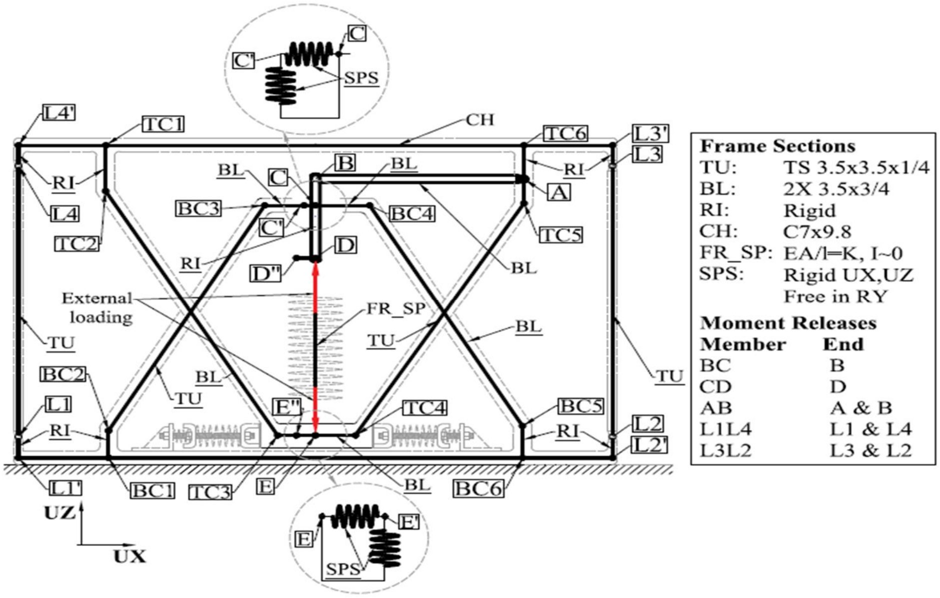

Fig. 1.5: Detailed model of NSD in program SAP2000

The frame element assembly $D'' - D - E - E''$ needs to deform as a rigid body with the rotations at all joints being calculated as the rigid body rotation of the spring. In order to achieve zero relative rotation between the spring and the supplemental frame elements ($D - D''$ and $E - E''$), the supplemental frame elements need to be rigid. Moreover, the spring frame element must have small but non-zero bending stiffness so that it allows for unrestricted rotation of the supplemental frame elements (D $-$ D'' and $E - E''$). To ensure that the joint rotations are equal to the rigid body rotation of the spring, special detailing must take place at the connections of the spring on top and bottom. At point D free rotation between member CD and member DE must be allowed and the rotation at point D must be equal to the rigid body rotation of the spring (member DE). In order to achieve this, a moment release must be specified at joint D for member CD but not for member DE. The pivot plate is modelled as two rigid beam elements that merge into point C. In order to model the connection between the pivot plate and the bottom chevron at point C, an additional joint C' is introduced at the location of joint C. The two joints are connected with stiff axial springs in order to ensure equal translations but independent rotations while the continuity of the bottom chevron is maintained.

F. Modeling of Superstructure in SAP2000 v21

The superstructure, G+10, G15 and G+20 multi storied RCC structures are modeled with bay width 3m in both X and Y direction with and without the application of NSD and GSA. The material properties and sections utilized for the modeling of RCC structures are mentioned in Table.

Parameters	Data
Thickness of Slab	125mm
Height of G+10 RCC structure	38.5m
Size of Beam	300 mm x 300 mm
Size of Column	300 mm x 300 mm
Grade of Concrete	M30
Grade of Steel	Fe415
Live load on Floor	3 KN/m^2
Live load on Roof	1.5 KN/m^2
Floor Finish	1 KN/m^2
Floor to Floor Height	3.5 m

International Journal for Research in Applied Science & Engineering Technology (IJRASET)
ISSN: 2321-9653; IC Value: 45.98; SJ Impact Factor: 7.538
Volume 11 Issue XII Dec 2023- Available at www.ijraset.com

II. RESEARCH AIM AND OBJECTIVE

A. Aim

The aim of the research is to study the role of structural control system to enhance the overall structural performance under seismic excitation. The present work is focused to study and find the different parameters viz., Base Shear, Roof Displacement, Roof Acceleration, and Column Force which are acting as a measure of seismic performance of RCC moment resisting framed structure using Negative Stiffness Device as Base Isolation and Distributed Isolation.

B. Objectives

1) To model the NSD in SAP2000.
2) To study and compare the position of NSD as Base Isolation and Distributed Isolation.
3) To study the effect of previous ground acceleration on response of structure.
4) To study the behavior of the building by changing height of structure under different earthquakes.
5) To study and compare the parameters such as Base Shear, Roof Displacement, Roof Acceleration and Column Force.

III. PROBLEM STATEMENT

From the literature survey it is observed that negative stiffness device is very advantageous for control of the structures in the event of an earthquake. But until now NSD has been used for bridge structures and base isolated structures only. In the present study Negative Stiffness Device is used for reducing the effects of an earthquake in High Rise RCC buildings by using at various floors.

The present study has investigated the response of three multi story RCC buildings viz., G+10, G+15 and G+20 storey RCC building. All the Multi Storey RCC structures are analyzed for 5 bays, each in X and Y direction with bay width 3m. All the models are analyzed for a constant storey height of 3.5m. Also, all the models are analyzed for two combinations such as with and without the application of NSD+GSA under the action of four real time histories viz., Imperial Valley (El Centro) (1940), Bhuj (India) (2001), Uttarkashi (India) (1991), Dharmshala (India) (1986). The RCC model in SAP2000 v21 is analyzed for the parameters such as base shear, roof acceleration, roof displacement and column force under all considered earthquakes.

IV. METHODOLOGY

In the first phase of the study a Negative Stiffness Device is first modeled in SAP2000 and G+10 RCC building is analyzed and validated with results available in the considered paper.

In the second phase of the study the RCC multi storey G+10, G+15 and G+20 structures are modeled and analyzed for all the combinations mentioned above under all the considered earthquakes. For all the structures considered in the study Negative stiffness device is applied in the 1st, 3rd and 5th bay along X direction and in all the frames along Y direction at first floor level in base isolated structure as shown in fig. 3.1. and for distributed isolation NSD's are placed at alternate floors in two ways as Core Isolation and External Isolation as shown in fig. 3.2 and fig. 3.3. The RCC Building is designed as per I.S. 456:2000 and the loads are applied as per IS: 875.

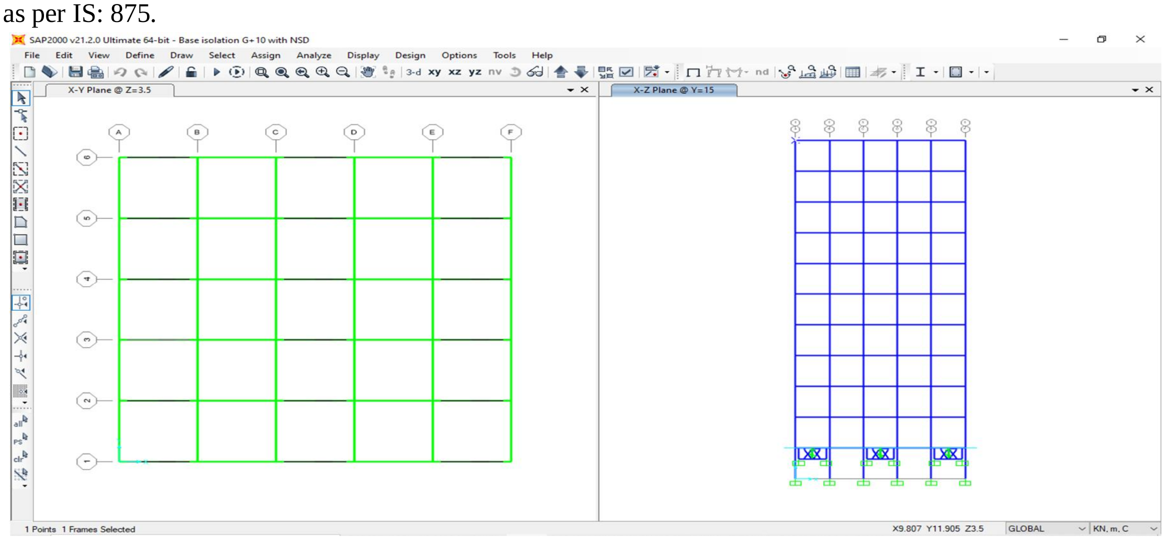

Fig. 3.1 Plan and Elevation of G+10 storied RCC Base Isolated structure

ISSN: 2321-9653; IC Value: 45.98; SJ Impact Factor: 7.538
Volume 11 Issue XII Dec 2023- Available at www.ijraset.com

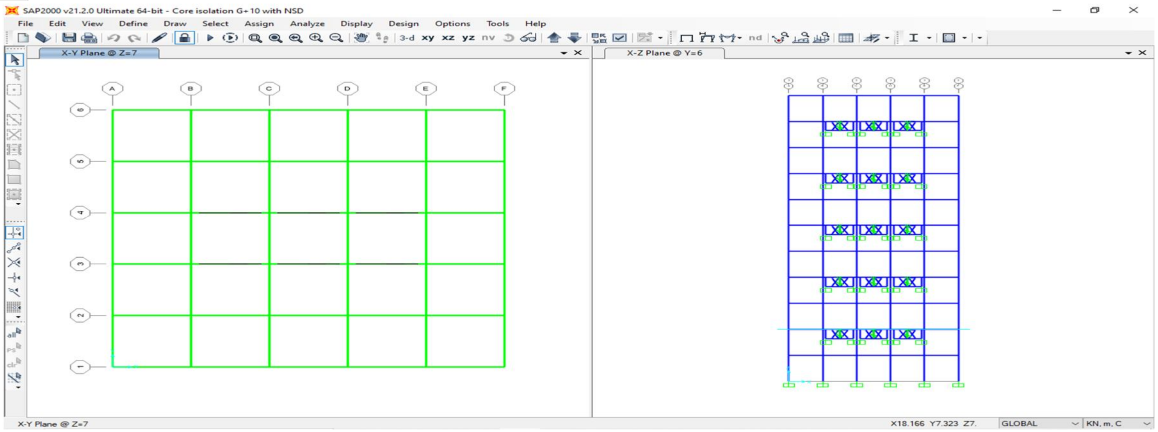

Fig. 3.2 Plan and Elevation of G+10 storied RCC Core Isolated structure

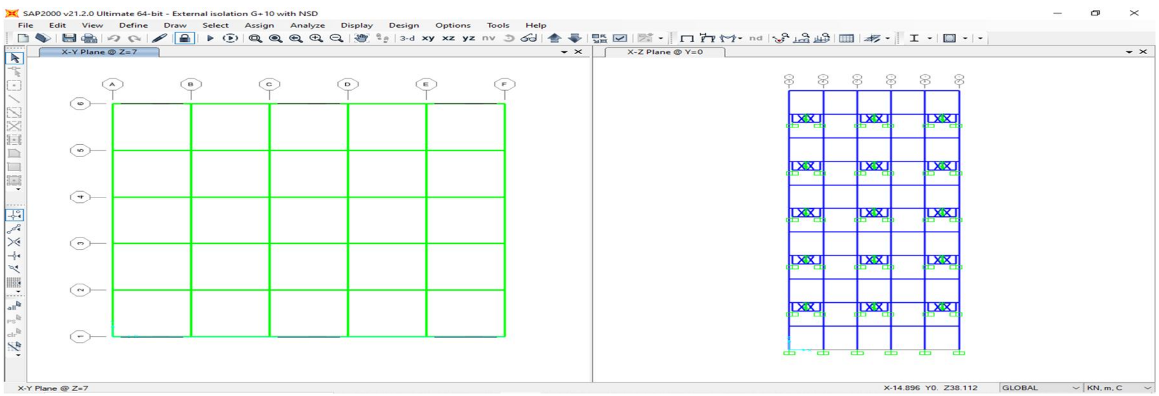

Fig. 3.3 Plan and Elevation of G+10 storied RCC Externally Isolated structure

V. RESULTS

A. Results

The results of Base Shear, Roof Acceleration, Roof Displacement and Column Force obtained from the analysis of G+10, G+15 and G+20 storied RCC structures with and without the application of NSD under the action of considered four earthquakes are presented in this section.

Table 5.1 % variation in base shear obtained for G+10, G+15 and G+20 storey structure

Ht. of Str.	Earthquake	Base Shear (kN)						
		Without NSD	With NSD as					
			Base Isolation	% Vari.	Core Isolation	% Vari.	External Isolation	% Vari.
G+10	EL-CENTRO	465.596	463.6	-0.42	520.2	11.73	580.2	24.61
	BHUJ	38.1	37.5	-1.57	40.2	5.51	43.2	13.41
	DHARMASHALA	490.145	465.2	-5.09	565.2	15.31	689.2	40.61
	UTTARKASHI	147.48	144.8	-1.83	157.8	7.00	175.2	18.80
G+15	EL-CENTRO	585.147	573.0	-2.08	622.5	6.38	702.5	20.06
	BHUJ	44.041	43.2	-1.88	45.1	2.40	47.8	8.54
	DHARMASHALA	629.348	583.5	-7.28	680.2	8.08	762.5	21.16
	UTTARKASHI	176.796	167.2	-5.43	183.2	3.62	198.5	12.28
G+20	EL-CENTRO	593.174	548.3	-7.57	628.5	5.96	670.1	12.98
	BHUJ	47.271	46.5	-1.64	48.3	2.07	50.1	5.98
	DHARMASHALA	778.503	701.8	-9.85	830.3	6.65	890.3	14.35
	UTTARKASHI	199.312	188.2	-5.58	203.5	2.10	220.3	10.53

ISSN: 2321-9653; IC Value: 45.98; SJ Impact Factor: 7.538
Volume 11 Issue XII Dec 2023- Available at www.ijraset.com

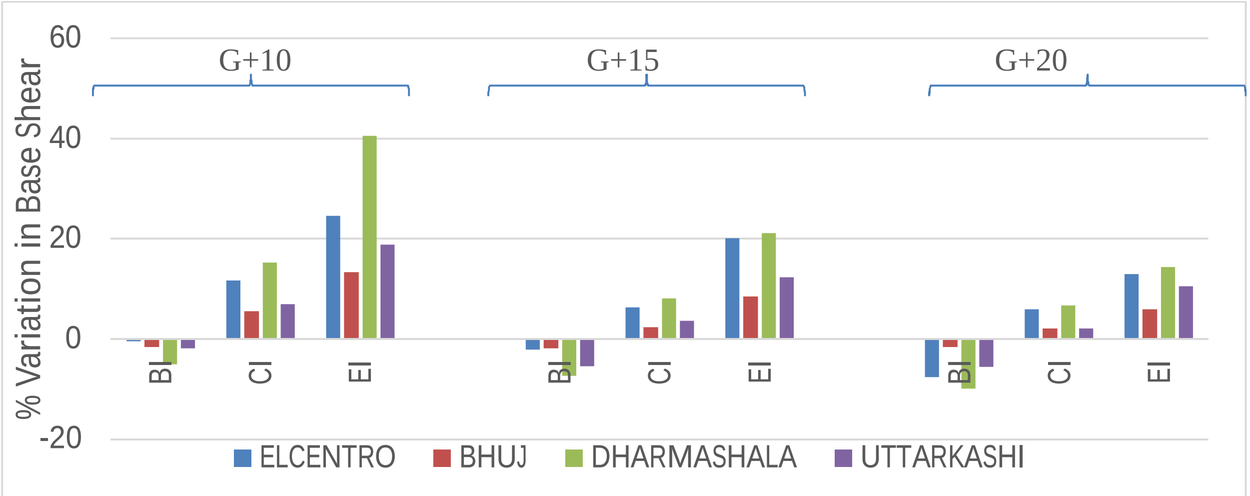

Fig. 5.1 Graph of % Variation in Base Shear for G+10, G+15 and G+20 storey structure subjected to different earthquakes

Table 5.2 % variation in roof acceleration obtained for G+10, G+15 and G+20 story structure

Ht. of Str.	Earthquake	Roof Acceleration (m/s^2)						
		Without NSD	With NSD as					
			Base Isolation	% Vari.	Core Isolation	% Vari.	External Isolation	% Vari.
G+10	EL-CENTRO	1.96	2.07	5.6	3.92	100.0	3.75	91.3
	BHUJ	0.32	0.36	12.5	0.49	53.1	0.48	50.0
	DHARMASHALA	2.63	2.69	2.3	4.29	63.1	4.28	62.7
	UTTARKASHI	0.86	0.87	1.2	1.48	72.1	1.49	73.3
G+15	EL-CENTRO	1.61	1.66	3.1	4.88	203.1	4.8	198.1
	BHUJ	0.28	0.29	4.4	0.32	15.2	0.31	11.6
	DHARMASHALA	2.11	2.31	9.7	2.72	29.1	2.64	25.3
	UTTARKASHI	0.64	0.67	4.7	1.38	115.6	1.33	107.8
G+20	EL-CENTRO	1.10	1.05	-4.5	4.22	283.6	3.9	254.5
	BHUJ	0.34	0.3	-11.8	0.38	11.8	0.36	5.9
	DHARMASHALA	2.04	2	-2.0	3.04	49.0	3.02	48.0
	UTTARKASHI	0.67	0.64	-4.5	1.56	132.8	1.44	114.9

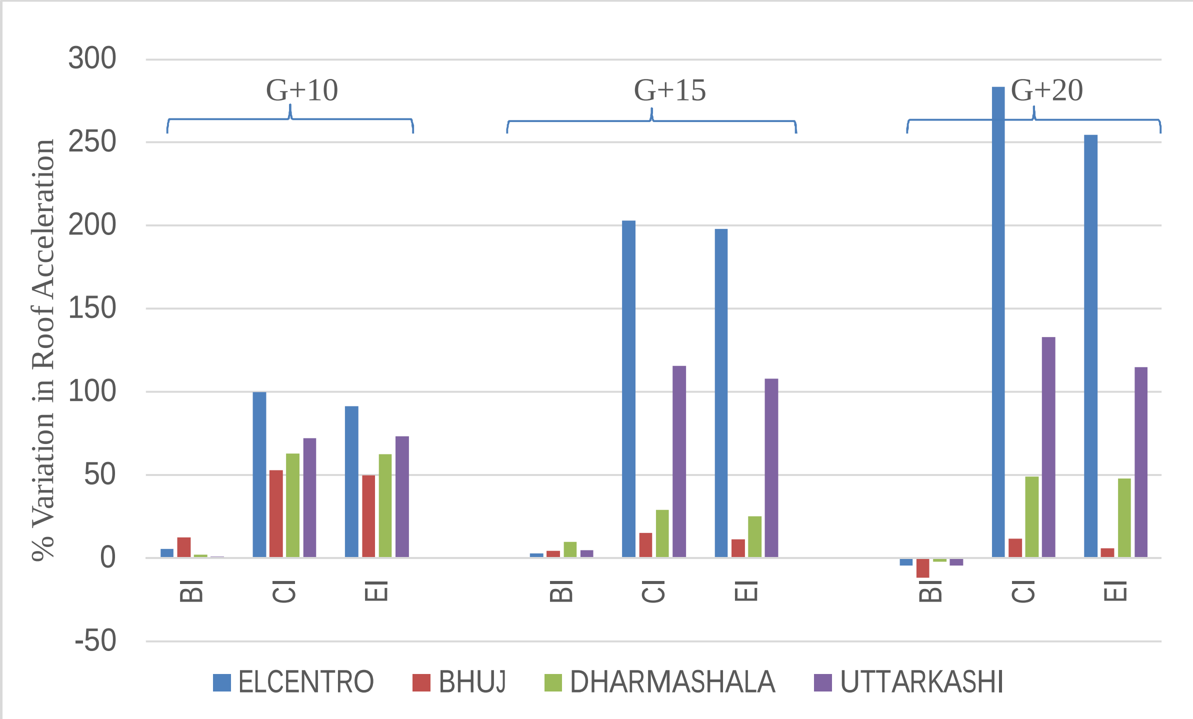

Fig. 5.2 Graph of % Variation in Roof Acceleration for G+10, G+15 and G+20 storey structure subjected to different earthquakes

Table 5.3 % variation in roof displacement obtained for G+10, G+15 and G+20 story structure

Ht. of Str.	Earthquake	Roof Displacement (mm)						
		Without NSD	With NSD as					
			Base Isolation	% Vari.	Core Isolation	% Vari.	External Isolation	% Vari.
G+10	EL-CENTRO	37.32	31.905	-14.5	19.128	-48.7	18.896	-49.4
	BHUJ	6.45	5.85	-9.3	3.115	-51.7	3.08	-52.2
	DHARMASHALA	31.679	28.899	-8.8	11.728	-63.0	11.657	-63.2
	UTTARKASHI	8.502	6.761	-20.5	6.712	-21.1	6.598	-22.4
G+15	EL-CENTRO	57.337	53.174	-7.3	21.313	-62.8	20.477	-64.3
	BHUJ	4.48	4.42	-1.3	2.1	-53.1	1.98	-55.8
	DHARMASHALA	35.867	34.56	-3.6	5.505	-84.7	5.05	-85.9
	UTTARKASHI	8.011	7.915	-1.2	5.21	-35.0	4.721	-41.1
G+20	EL-CENTRO	58.846	58.732	-0.2	21.764	-63.0	19.163	-67.4
	BHUJ	4.64	4.6	-0.9	2.087	-55.0	1.044	-77.5
	DHARMASHALA	57.575	56.21	-2.4	6.145	-89.3	5.987	-89.6
	UTTARKASHI	11.185	11.111	-0.7	6.841	-38.8	6.213	-44.5

International Journal for Research in Applied Science & Engineering Technology (IJRASET)
ISSN: 2321-9653; IC Value: 45.98; SJ Impact Factor: 7.538
Volume 11 Issue XII Dec 2023- Available at www.ijraset.com

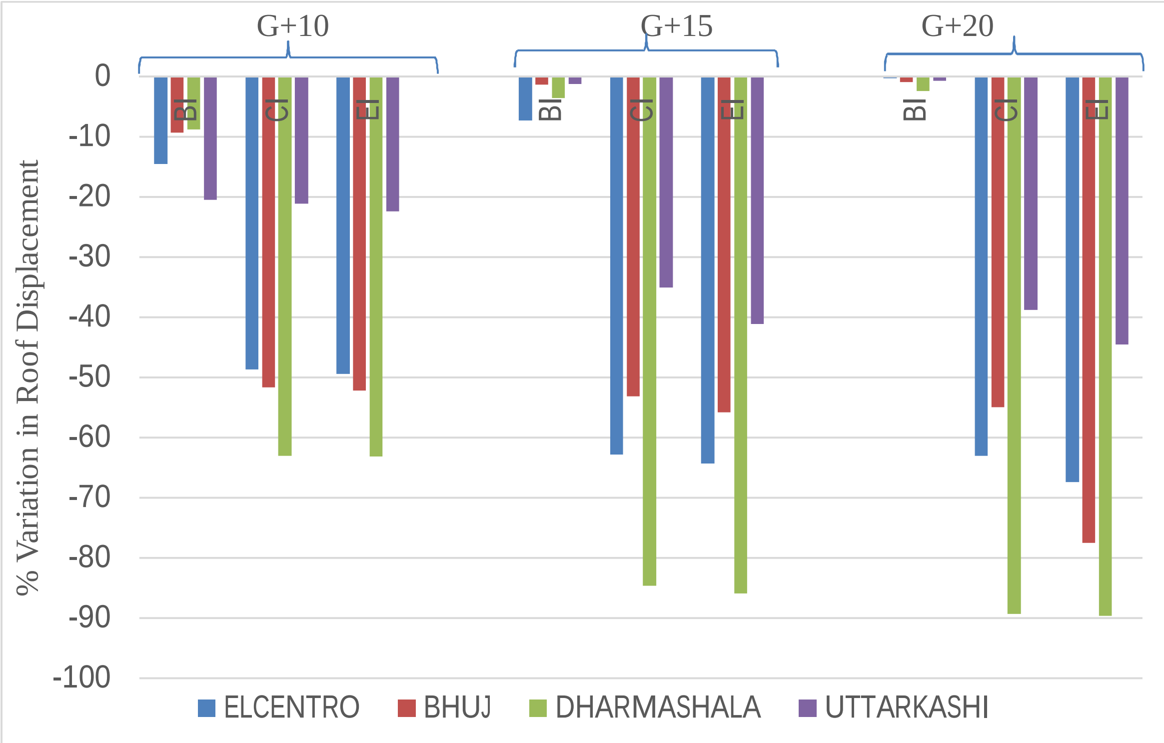

Fig. 5.3 Graph of % Variation in Roof Displacement for G+10, G+15 and G+20 storey structure subjected to different earthquakes

Table 5.4 % variation in column force obtained for G+10, G+15 and G+20 story structure

Ht. of Str.	Earthquake	Column Force (kN)						
		Without NSD	With NSD as					
			Base Isolation	% Vari.	Core Isolation	% Vari.	External Isolation	% Vari.
G+10	EL-CENTRO	541.197	647.443	19.6	582.644	7.7	466.076	-13.9
	BHUJ	418.331	530.898	26.9	520.164	24.3	403.4	-3.6
	DHARMASHALA	533.049	636.473	19.4	555.287	4.2	455.385	-14.6
	UTTARKASHI	439.36	551.225	25.5	536.629	22.1	422.3	-3.9
G+15	EL-CENTRO	835.481	1018.288	21.9	855.35	2.4	670.298	-19.8
	BHUJ	679.58	863.531	27.1	746.561	9.9	643.442	-5.3
	DHARMASHALA	760.372	946.539	24.5	767.848	1.0	661.943	-12.9
	UTTARKASHI	700.65	885.789	26.4	758.051	8.2	655.137	-6.5
G+20	EL-CENTRO	1087.575	1346.781	23.8	956.691	-12.0	783.018	-28.0
	BHUJ	961.425	1270.8	32.2	916.22	-4.7	850.687	-11.5
	DHARMASHALA	1133.057	1430.2	26.2	936.125	-17.4	863.042	-23.8
	UTTARKASHI	991.646	1287.4	29.8	929.341	-6.3	859.113	-13.4

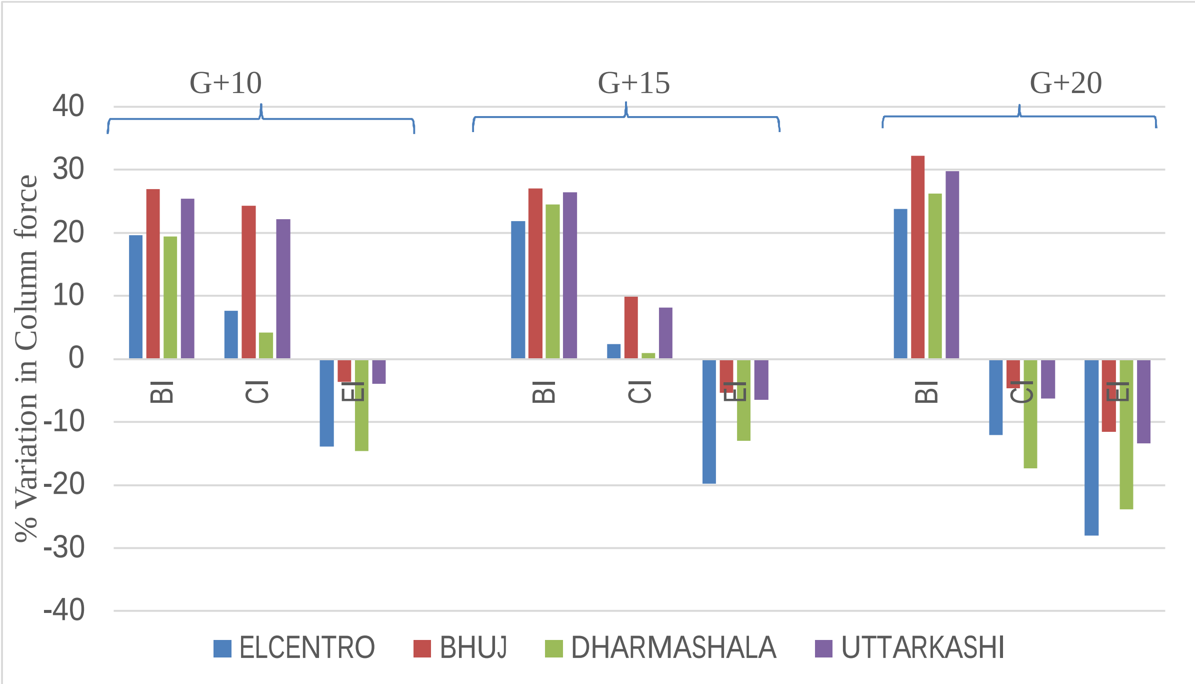

Fig. 5.4 Graph of % Variation in Column Force for G+10, G+15 and G+20 storey structure subjected to different earthquakes

B. *Summary of Results*

Table 5.5 *Summary of Results*

Sr. No.	Parameter	Maximum Reduction		Earthquake	Type of Structure
		In case of	% Reduction		
1	Base Shear	Base Isolation	9.85	Dharmshala (1986)	G+20
2	Roof Acceleration	Base Isolation	11.8	Bhuj (2001)	G+20
3	Roof Displacement	External Isolation	89.6	Dharmshala (1986)	G+20
4	Column Force	External Isolation	23.8	Dharmshala (1986)	G+20

C. *Discussion on Summary of Result*

1) Base isolation is effective in reducing base shear as compared to distributed isolation in a seismic analysis because base isolation allows the building to move relative to the ground and effectively reducing the amount of seismic energy transmitted to the structure thus reducing the maximum base shear. Base isolation reduces maximum base shear by decoupling the building from the ground motion and absorbing the seismic energy.

2) Roof acceleration in a base isolated structure is reduced because in that, NSD serve to decouple the building's structure from the ground motion. During an earthquake, the isolation devices absorb and dissipate a significant portion of the seismic energy, reducing the amount of energy that is transmitted to the building's structure. This reduction in seismic energy results in a lower roof acceleration.

3) External isolation reduces the maximum displacement as compared to core isolation in a seismic analysis because external isolation provides a larger area for energy dissipation and reducing the displacement of the structure.

4) External isolation reduces the maximum column force as compared to core isolation in a seismic analysis because external isolation provides a larger area for energy dissipation and reduces lateral load due to earthquake and ultimately reducing the forces on the columns. Also, external isolation can reduce the deformations of the structure during seismic events, leading to reduced column forces.

VI. CONCLUSION

1) The value of base shear for particular height of building depends on earthquakes PGA and period of structure. In case of base isolated structure base shear value decrease because base isolation allows the building to move relative to the ground and effectively reducing the amount of seismic energy transmitted to the structure and reducing the maximum base shear. The value of base shear decreases by maximum 9.85% for G+20 structure subjected to Dharmshala earthquake. In case of distributed isolation value of base shear increases continuously as the height of structure is increased. For Base shear reduction, base isolation has observed to be effective for all three structures.
2) Value of roof acceleration for particular height of building changes with different type of earthquake because the value of peak ground acceleration is different for different earthquake. Roof acceleration is seen maximum (2.63 m/s^2) for Dharmshala earthquake for which PGA value is maximum (1.42 m/s^2) and roof acceleration is minimum (0.32 m/s^2) for Bhuj earthquake for which PGA value is minimum (0.21 m/s^2). So, we can say that earthquake having maximum PGA causes higher roof acceleration.
3) Value of roof displacement for particular height of building changes with different type of earthquake. Roof displacement is seen maximum (58.846 mm) for Dharmshala earthquake for which PGA value is maximum and is minimum (4.48 mm) for Bhuj for which PGA value is minimum. So, the earthquake having maximum PGA causes higher roof displacement. With increase in height, value of roof displacement increases for all earthquakes because as we go for higher storey height due to lateral excitation value of roof displacement increases.
4) The value of column force is maximum (1133.057 kN) for Dharmshala earthquake which is having maximum PGA and for Bhuj earthquake is minimum (418.331 kN) for same height of building and for different height it increases as storey height increases because of self-weight, loading on structure and lateral excitation due to earthquake.
5) For Base shear reduction, base isolation has observed to be effective for all three structures.
6) For distributed isolation structure value of roof acceleration continuously increases with increase in storey height for all considered earthquakes.
7) For base isolated structure as height of structure increases % reduction in roof displacement decreases, so it is less effective for reducing roof displacement of high-rise structure. In case of distributed isolation % reduction in roof displacement increases as storey height increases so, as compared to base isolation; distributed isolation is very much effective in reducing top story displacement.
8) For base isolated structure column force on considered column increases as height of structure increases for all considered earthquakes and in case of core isolation for G+10 and G+15 its value increases but thereafter for G+20 it gets decreased. For external isolation, force on column decreases continuously as height of structure is increased because of NSD's position for that case is around periphery of structure which helps in reducing vibrations effectively and ultimately reduces column force.

REFFERENCES

[1] A. Sarlis, D. T. R. Pasala,(2012) "Negative Stiffness Device for Seismic Protection of Structures". Journal of Structural Engineering, ASCE, volume139, No. 7.
[2] Tong Sun, Zhilu Lai, Satish Nagarajaiah, (2016) "Negative stiffness device for seismic protection of smart base isolated benchmark building". Structural Control Health Monitoring, WILEY
[3] A.A. Sarlis , D. T. R. Pasala , (2016) "Negative Stiffness Device for Seismic Protection of Structures: Shake Table Testing of a Seismically Isolated Structure". Journal of Structural Engineering, ASCE, volume142, No.5.
[4] D. T. R. Pasala , A. A. Sarlis , (2013) "Adaptive Negative Stiffness: New Structural Modification Approach for Seismic Protection". Journal of Structural Engineering, ASCE, volume139, No. 7.
[5] Onkar Paril, Dr. S.N. Tande, Dr. A. B. Kulkarni, (2016) "Concept of Negative Stiffness Device for R.C. Buildings in Seismic Areas". International Journal of Latest Trends in Engineering and Technology , Volume 7.
[6] Gisha Mary Mathew , R. S. Jangid (2018), "Seismic response control of a building by negative stiffness devices". Asian Journal of Civil Engineering, Springer.
[7] Hong-Nan Li, Tong Sun, Zhilu Lai, Satish Nagarajaiah (2018), "Effectiveness of Negative Stiffness System in the Benchmark Structural-Control Problem for Seismically Excited Highway Bridges". Journal of Bridge Engineering , ASCE ,Volume 23 , No.3.
[8] D. T. R. Pasala, A. A. Sarlis (2013), "Simulated Bilinear-Elastic Behavior in a SDOF Elastic Structure Using Negative Stiffness Device: Experimental and Analytical Study". Journal of Structural Engineering, ASCE, Volume 140, No. 2.
[9] Amit H. Raheja, M.V. Waghmare (2015), "Seismic Analysis of High-Rise Building Using Negative Stiffness Device". International Journal of Advance Foundation and Research in Science & Engineering, Volume 1
[10] S. Nagarajaiah and S. Narasimhan (2006), "Smart base-isolated benchmark building. Part ii: phase 1 sample controllers for linear isolation systems," Structural Control and Health Monitoring, 2006, vol. 13, no. 2-3.
[11] Hirokazu lemura and Mulyo Harris Pradono (2003), "Pseudo Negative Stiffness Control of the Benchmark Cable-Stayed Bridge", Journal of Structural Control, Vol. no. 10, July 2003.

[12] A. A. Sarlis, D.T. R. Pasala, Michael C. Constantinou, Andrei M.Reinhorn, Satish Nagarajaiah and Douglas P. Taylor (2013), “Negative Stiffness for seismic protection of structures”, Technical Report MCEER-13-0005, 12 June 2013.
[13] SAP2000 CSI Analysis Reference Manual, Computer and Structures, Inc., Berkeley 2011.
[14] IS 456:2000, “Plain and Reinforced Concrete - Bureau of Indian Standards, New Delhi, India Code of Practice”.
[15] IS: 875(Part 2) - 1987 (Reaffirmed 2003), “Code of Practice for Design Loads (Other than Earthquake) for Buildings and Structures”, Bureau of Indian Standards, New Delhi, India.
[16] IS 1893 (Part 1): 2002, "Criteria for Earthquake Resistant Design of Structures Part 1 General Provisions and Buildings", Bureau of Indian Standards, New Delhi, India

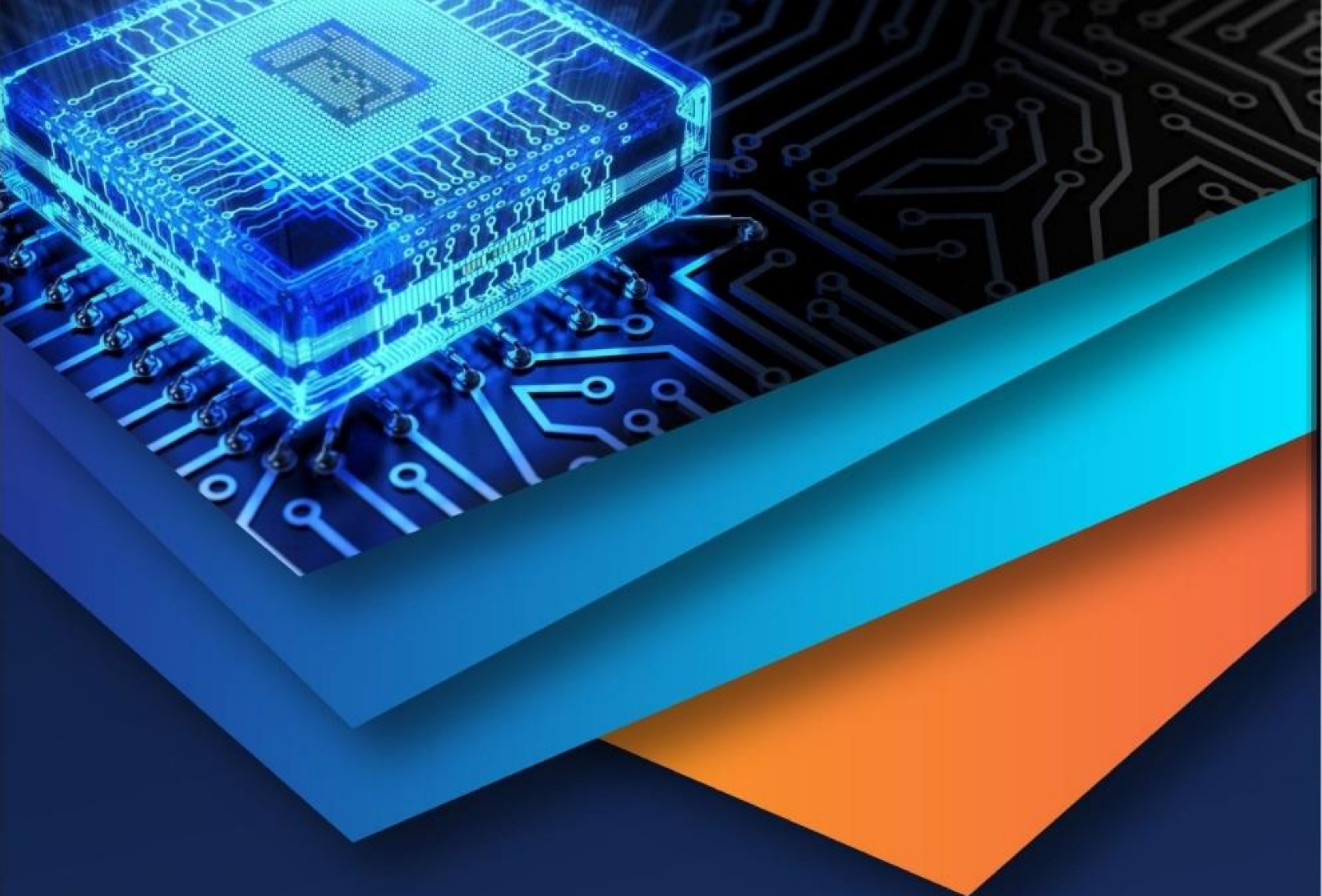

10.22214/IJRASET

45.98

IMPACT FACTOR:
7.129

IMPACT FACTOR:
7.429

INTERNATIONAL JOURNAL FOR RESEARCH

IN APPLIED SCIENCE & ENGINEERING TECHNOLOGY